IEEE Access
Multidisciplinary ⋮ Rapid Review ⋮ Open Access Journal

Received December 9, 2020, accepted January 29, 2021, date of publication February 24, 2021, date of current version March 15, 2021.

Digital Object Identifier 10.1109/ACCESS.2021.3062143

Three-Phase Transformer Inrush Current Reduction Strategy Based on Prefluxing and Controlled Switching

YUANLIN PAN[1], XIANGGEN YIN[1], (Member, IEEE), ZHE ZHANG[1], BINYAN LIU[1], MAOLIN WANG[1], AND XIN YIN[2], (Member, IEEE)

[1]State Key Laboratory of Advanced Electromagnetic Engineering and Technology, Huazhong University of Science and Technology, Wuhan 430074, China
[2]Department of Electrical Engineering and Electronics, University of Liverpool, Liverpool L69 3GJ, U.K.

Corresponding author: Xin Yin (leoxinyin@qq.com)

This paper is supported by the National Key Research and Development Plan of China (2016YFB0900600).

ABSTRACT Inrush current with high amplitude is generated when the transformer is energized. On the one hand, it will have a negative impact on the safety of the transformer itself, and even cause the relay protection to malfunction. On the other hand, it may reduce operation speed of the protection when there is slight fault because of the protection restraint criteria. Both aspects will affect grid security. Based on the generation mechanism of inrush current, this paper proposes an inrush current reduction strategy that combines prefluxing and controlled switching technology. By constructing an equivalent magnetic circuit model of the large-capacity three-phase transformer with a universal core structure, the analytical formulas of the magnetic flux at each stage of implementing the strategy are obtained, and then the parameters design method of this strategy is proposed. The accuracy of the theoretical analysis of magnetic flux is verified through the accurate simulation. Compared with common inrush current reduction strategies, this strategy can reduce the inrush current to 0.5 times rated current below in any situation where the residual flux is unknown and the ''core flux equalization'' effect are not obvious, avoiding the problem of residual flux measurement. Finally, in the case of the transformer differential protection, the influence of this strategy on the protection is analyzed from the perspective of theory and simulation, and it shows that it can improve the performance of various protections effectively.

INDEX TERMS Inrush current reduction, residual flux, equivalent magnetic circuit, prefluxing, controlled switching, differential protection.

I. INTRODUCTION

Power transformer, especially large-capacity transformer plays an important role in power transmission, and its operating characteristics have an important impact on the stable operation of the transformer itself and the power system. In order to reduce the size of large-capacity transformers, three phases transformer with five columns core or single phase core is often used. In the connection of transformer winding, Y_0/Δ is the most common type.

When unloaded the power transformer is energized, due to the transient characteristics of the magnetic flux and the non-linear characteristics of the core material, inrush current with a considerable amplitude will be generated. The maximum peak value of the inrush current may reach about 10 times the rated current of the transformer, and the duration time may be as long as several seconds [1]–[3], which may cause damage to the transformer. At the same time, the large inrush current and the sympathetic inrush generated by interaction between transformer and its adjacent operating transformer may cause the main protection of the transformer, generator and the adjacent line to malfunction [4]. Especially in recent years, serious accidents such as misoperation of the busbar connection protection and even the zero-sequence backup protection of the upper-level line during the power transformer energization. It shows that the large zero-mode inrush current generated by the transformer prefluxing inrush current is the direct cause of the misoperation [5], [6]. Therefore, the way of reducing the inrush current to ensure the safety of the transformer itself and improve the protection performance has been highly valued by scholars.

The associate editor coordinating the review of this manuscript and approving it for publication was Xue Zhou.

Inrush current is the current caused by magnetic flux saturation and core saturation characteristics. Its characteristics are related to factors such as the initial phase angle of the voltage, the residual flux, and the hysteresis characteristic [7]–[9]. For a three-phase transformer, the connection of the winding and the core structure must be considered too. Researches have put forward methods to reduce inrush current, which can be mainly divided into two types: controlled switching and switching inrush current suppressor. The principle of controlled switching is that the appropriate closing angle is selected to weaken the transient magnetic flux so that it does not exceed the saturation valve. This technology is currently widely used. The traditional controlled switching strategies mainly includes rapid closing strategy, delayed closing strategy and simultaneous closing strategym [1], [10], [11]. Among them, the rapid closing strategy is that one phase is closed at first, and the other two phases are closed 1/4 cycle later. However, the premise of the strategy is that the three-phase residual flux is known. The simultaneous closing strategy is only applicable to specific three-phase residual flux modes of transformers. For the delayed closing strategy, the residual flux of one phase is needs to know at least. After the phase with known residual flux is closed, the other phases are closed after a few cycles later according to the ''core flux equalization'' effect.

A method to obtain the residual flux of the core proposed using LabVIEW [12]. Regarding the measurement of residual flux. This method requires that the measuring device is always running on the network. Generally, the residual flux of the iron core after the circuit breaker is opened can be measured. However, for the first time the transformer is put into operation, or the transformer is overhauled, or the DC resistance test is performed, and due to the special changing law of the residual flux, the accurate measurement of the residual flux under various working conditions has always been a technical problem [3], [13]–[16].

These three closing control strategies all need to obtain at least one phase residual flux in advance. However, due to the special law of residual flux, the measurement of residual flux has always been a technical problem For this problem, it is proposed a simple controlled switching strategy [17] assuming that the residual flux is in the worst case to design the closing angle, so the residual flux may not be needed. The actual effect is that the inrush current can be reduced to below 46.7% of the maximum inrush current, so the reduction effect is not significant. It is proposed to determine the closing sequence and time by controlling the opening sequence and time of the three-phase circuit breaker. This method requires that the opening of the circuit breaker is controllable. However, the wrong opening of the circuit breaker may bring serious consequences, so this method is difficult to be realized in engineering.

In addition to the residual flux, the optimal closing time in controlled switching is often related to the core structure type and winding connection form. It is analyzed the magnetic flux of the three-phase three-legged stacked-core power transformers with Y/Y-connected winding during the closing process, so as to obtain the optimal closing angle [18]. However, the flux coupling between three phases is not considered in flux calculation, and the method also depends on the accurate measurement of residual flux. Based on the duality transformation between electric and magnetic circuits [19], a circuit model of three phases transformer with single phase cores and Y_0/Δ-connected transformer that is considered coupling among phases is established. This modeling method for obtaining magnetic flux can be extended to solve the magnetic flux of transformers with other structures and it has universal applicability. However, in the modeling, this article only considered the saturation characteristics of the iron core. And corresponding strategy is proposed assuming that the three-phase magnetic flux has ''core flux equalization'' effect. It is fail to consider that the possibility that magnetic flux ''core flux equalization'' may be insignificant, which may result in a failure of the strategy. It is considered that there is ''core flux equalization'' effect in Δ-connected transformer, that is, after a certain phase is closed, the transient magnetic flux of the other two phases will rapidly decay to equilibrium, so the delayed closing strategy can be adopted. However, the strategy fails to consider the possibility that the ''core flux equalization'' effect may not be obvious. At present, there is no research report on the application of controlled switching in inrush current reduction of three phases transformer with five columns core or single phase core. Therefore, in the research of controlled switching strategy, how to avoid the problem of accurate measurement of residual flux, consider the core structure and characteristics of three phases large capacity transformer with five columns core or single phase core, model and analyze the magnetic flux in the process of closing, and put forward the optimal closing strategy are needed to be in-depth research.

The principle of reduction of inrush current by switching inrush current suppressor is that the transient magnetic flux of transformer is reduced as much as possible by switching voltage control equipment or prefluxing equipment. The method of switching prefluxing transformer is that the prefluxing transformer is put into operation first, and then the transformer is energized after the magnetic flux is stable. Finally, the prefluxing transformer is bypassed. This method is mainly used in ship power system. However, the inrush reduction effect of this method will be affected by residual flux. In reference [6], switching power electronic equipment can realize the voltage rising slowly by controlling the trigger angle of thyristor. It can be applied to the inrush current reduction of large-capacity transformer. The reduction effect will not be affected by residual flux. However, it is complicated that the strategic design involves power electronic equipment control.

The main inrush current reduction principle of switching the prefluxing equipment is that the initial magnetic flux of the transformer is set as a certain expected value by prefluxing before the transformer is energized, and then the magnetic flux control can be realized by using the controlled

switching. DC current is mainly used to preflux at present research. In other words, the magnetic flux of the transformer is set as saturation value by charging DC current in the primary side of the transformer, and then the optimal closing control angle can be obtained. This method is used in a single-phase transformer, and the prefluxing current is generated by the designing capacitor. The inrush current reduction effect of the strategy is significant [14]. The strategy avoids the problem of residual flux measurement at the same time. The method provides possibilities for the inrush current reduction of more widely used three-phase transformers.

However, this document estimates the prefluxing current as the no-load current level of transformer, and the effectiveness of the prefluxing current is demonstrated through simulation and experiments. But design of the prefluxing current is lacked the necessary theoretical analysis for parameter. For large three-phase transformers, especially three phases and five columns transformer and a Y_0/Δ-connected winding, the three-phase magnetic fluxes are mutually coupled. Moreover, when the three-phase magnetic flux generated by the primary current of the transformer is unbalanced, current will be generated in the closed triangular connected winding, which affect the primary current in turn. Therefore, the three-phase magnetic fluxes will affect each other during the prefluxing process for this kind of transformer, and the required prefluxing parameters cannot be deduced by simple equivalent of the previously studied single-phase transformer. Therefore, in order to accurately design the parameters such as the prefluxing current that meet the requirements, it is necessary to remodel the Y_0/Δ-connected transformer that can consider the core structure and analyze the magnetic flux characteristics in the prefluxing process. In fact, the magnetic flux characteristics are also closely related to the hysteresis and saturation characteristics of the iron core. Its analysis requires solving nonlinear equations, which is also a difficult point in research.

In summary, for large-capacity transformers, it is a valuable work to propose an inrush reduce strategy that can avoid residual flux measurement and consider the structure and characteristics of the core. There are few related studies at present.

This paper constructs a large-capacity transformer magnetic circuit model. When solving the analytical expression of the flux linkage in the process of applying the strategy, the Y_0/Δ-connected winding mode and the hysteresis and saturation characteristics of the core are considered. And then, in order to meet the requirements of inrush current reduction, the parameters of the control strategy are designed through magnetic flux analysis. After that, simulation is used to verify the analysis, and the effects of different inrush current reduction strategies under various working conditions are compared, which shows that the strategy of this article has better ability to reduce inrush current. Finally, the differential protection is taken as an example to analyze. The result shows that this strategy can improve a variety of types of protection performance effectively.

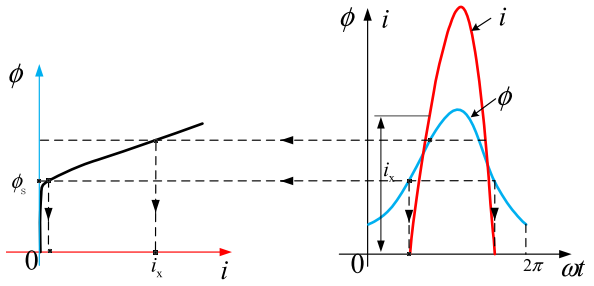

FIGURE 1. Schematic diagram of core excitation characteristics and inrush current generation principle.

II. INRUSH CURRENT REDUCTION STRATEGY BASED ON PREFLUXING AND CONTROLLED SWITCHING

The magnetic flux solution of large-capacity transformer during prefluxing and controlled switching process is the theoretical basis of inrush current reduction strategy design. Therefore, it is necessary to establish a transformer flux solution model first. The model should be able to consider the different core structures of large-capacity transformers, winding connection modes, core nonlinear characteristics, core residual flux, and the control parameters of the strategy such as prefluxing current and closing angle too. Therefore, in this section, the basic principle of inrush current reduction is briefly introduced first, and then a magnetic circuit model is established that can reflect the characteristics of the transformer above from the perspective of the magnetic circuit. On this basis, with the goal of designing an ideal three-phase magnetic flux, the influence of the control parameters on the magnetic flux characteristics is studied so as to propose a parameter design method to achieve the purpose of inrush current reduction. Finally, the inrush current reduction strategy is proposed.

A. PRINCIPLE AND STRATEGY OF INRUSH CURRENT REDUCTION

The root cause of the inrush current generated by the transformer lies in the non-linear excitation characteristics of the iron core, as shown in FIGURE 1. That is, when the transformer core is not saturated, the excitation inductance will be very large, and the required excitation current can be almost neglected at this time. When the magnetic flux in the iron core exceeds the saturation value, the magnetizing inductance will drop to the leakage inductance level, resulting in a larger inrush current.

The electromagnetic equation in the process of the single-phase transformer energized is following.

$$N\frac{d\phi}{dt} + iR = U_{\mathrm{m}}\sin(\omega t + \alpha) \tag{1}$$

In the equation, ϕ is the magnetic flux in the transformer core, i winding current, R is the sum of the system resistance and the transformer closing winding resistance, U_{m} is the system power supply amplitude, and α is the power initial phase angle at the time of closing.

By solving equation(1), the expression of magnetic flux ϕ can be solved as follows.

$$\phi = \frac{-LU_{\mathrm{m}}\cos(\omega t+\alpha)}{\sqrt{R^2+(\omega L)^2}} + \left(\phi_{\mathrm{in}} + \frac{LU_{\mathrm{m}}\cos\alpha}{\sqrt{R^2+(\omega L)^2}}\right) e^{-\frac{R}{L}t} \tag{2}$$

In the formula, L is the average inductance of the closing winding, and ϕ_{in} is the magnetic flux of the iron core before the transformer is closed, which is called the initial magnetic flux. The core magnetic flux consists of two parts: one part is a periodic component, and the other part is an attenuated aperiodic component. It can be seen that in addition to the parameter L determined by the transformer's own characteristics, and ϕ is mainly affected by R, α and the initial magnetic flux ϕ_{in}. Increasing the value of R can reduce the magnetic flux amplitude, which is mainly achieved through series resistance. However, the series resistance method alone is always not effective and needed to be coordinated with other means [20], [21]. So, the influence of ϕ_{in} and α on inrush current are mainly explored in this article.

Let $\phi_{\mathrm{m}} = \frac{LU_{\mathrm{m}}}{\sqrt{R^2+(\omega L)^2}}$, then ϕ_{m} is a certain value. When the initial phase angle α of the power supply takes different values, the maximum core magnetic flux will be different. Let $\phi_{\mathrm{p}} = \phi_{\mathrm{m}}\cos\alpha$. ϕ_{p} is called the prospective magnetic flux.

When $\phi_{\mathrm{in}} = -\phi_{\mathrm{p}}$, the maximum magnetic flux amplitude is the smallest, which is equal to ϕ_{m}, and the transformer goes into steady state directly after closing. At this time, the initial phase angle α of the power supply satisfies $\alpha = \pi\text{-arc}\cos\left(\frac{\phi_{\mathrm{in}}}{\phi_{\mathrm{m}}}\right)$. Since the saturation flux of the iron core is about $op\,(1.15-1.25)\,\phi_{\mathrm{m}}t$, there will be no inrush current under this condition.

When $\phi_{\mathrm{in}} \neq -\phi_{\mathrm{p}}$, and the ϕ_{in} is positive polarity, for example, the initial magnetic flux is equal to ϕ_{s}, the maximum value of the magnetic flux is ϕ_{s} if $\alpha = 180°$. The saturation value is not exceeded at this time, so there is almost no inrush current.

However, when $\phi_{\mathrm{in}} \neq -\phi_{\mathrm{p}}$, and the initial phase angle of the power supply is 0°, the maximum amplitude of the magnetic flux is $\phi_{\mathrm{in}}+2\phi_{\mathrm{m}}$. Under normal circumstances, the core residual flux ϕ_{r} will not exceed $0.85\phi_{\mathrm{m}}$ [1]. If the initial magnetic flux is residual flux, the maximum magnetic flux amplitude will be the maximum $2.85\phi_{\mathrm{m}}$ when $\phi_{\mathrm{in}} = 0.85\phi_{\mathrm{m}}$. When ϕ_{r} is negative, the maximum magnetic flux amplitude is $-2.85\phi_{\mathrm{m}}$. In both conditions, maximum magnetic flux is far greater than the saturation magnetic flux, and will cause very large inrush current. Therefore, the size of the initial magnetic flux ϕ_{in} and the initial phase angle α of the power supply at the time of closing have a great influence on the magnitude of the inrush current. If the proper initial magnetic flux and power initial phase angle can be selected, the inrush current can be effectively reduced.

The initial magnetic flux is not easy to obtain. First, because of the closed-loop core structure of the transformer core. Measurement equipment such as a flux meter cannot be used. Second, due to the special changing law of the residual

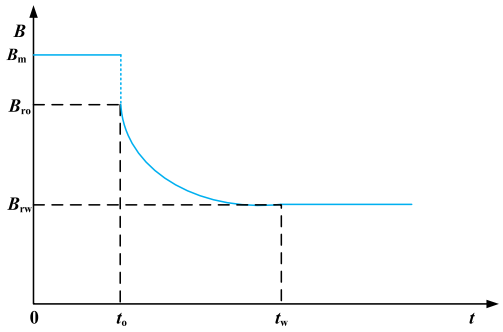

FIGURE 2. Change curve of residual flux.

flux of the transformer core. In the view of classical ferromagnetism, when the transformer winding is supplied with excitation current, the iron core will be subjected to the action of an external magnetic field, and the magnetic domains inside will be arranged in accordance with the direction of the magnetic field. Finally, a magnetic field B_{m} inside the iron core is formed, as shown in FIGURE 2. If the excitation current of the winding suddenly changes to zero at the time of t_{o}, for the magnetic domain losing the external constraint, some domains interact with the surrounding domains and tend to be disordered, and the domains concentrated in the same direction decrease. The macroscopic manifestation is that the magnetic induction intensity decreases rapidly to a certain state value. The residual flux of this state is defined as the initial residual flux B_{ro} (the intersection of B-H hysteresis loop and longitudinal axis). However, at this time, the energy of the core domain has not been reduced to the minimum. The direction of the magnetic domain will continually slowly confuse with the passage of time, leading to the further decrease of the magnetic flux, and the domain motion reaches a stable state after t_{w}. The residual flux state in the core is defined as the steady-state residual flux B_{rw} [14].

In the process that flux changes from initial residual flux to steady-state residual flux state, the magnetic domain moves slowly, and the voltage of core winding is almost zero. When the core residual flux reaches a stable state, the magnetic field state will not change, unless a new excitation current is applied to the winding.

The existing research methods of residual flux measurement are based on the on-line integration of voltage. In the actual situation, the voltage corresponding to the $t_{\mathrm{o}}-t_{\mathrm{w}}$ stage is almost 0, so it is difficult to measure the magnetic flux change. At present, the direct measurement of residual flux of transformer core is still a difficult problem in engineering. Therefore, this paper proposes the method that the core flux is prefluxed to the positive saturation value ϕ_{s} by DC current, so as to provide a certain initial flux, and then optimal closing angle can be selected to close. According to the basic principle of inrush current reduction, the optimal closing angle is 180 degrees.

The specific process of inrush current reduction strategy is as follows, which is mainly divided into two parts. First, A-

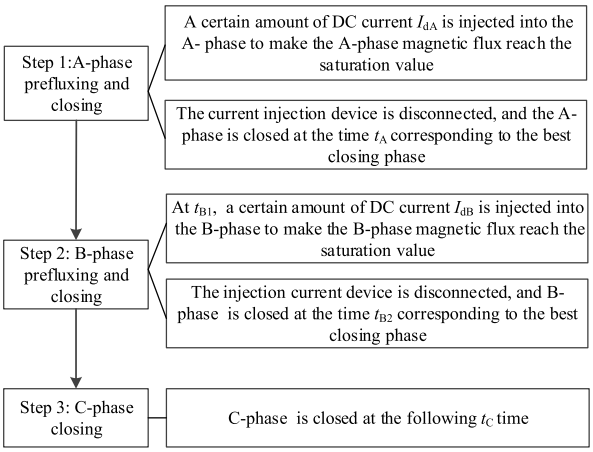

FIGURE 3. The inrush current reduction strategy based on prefluxing and controlled switching.

phase of the transformer is prefluxed to the positive saturation value. Secondly, the circuit breaker of this phase is closed at the initial phase angle of the power source at 180°. The same prefluxing and controlled switching strategy as A-phase is adopted to B-Phase. According to the balance of the three-phase magnetic flux, C-Phase magnetic flux will directly enter the steady-state without prefluxing. There is almost no inrush current when closing at any closing angle, which will be further analyzed later. Overall, almost no inrush current is generated during the entire closing process. Therefore, this strategy can be simply described to a ''phase-to-phase prefluxing and phase-to-phase controlled switching closing'' method. The reason that ''separate-phase prefluxing, three-phase closing at the same time'' method is not selected for the power phase angles of three phases meeting the symmetrical relationship of 120°. To completely eliminate inrush current, symmetrical relationship of 120° of the initial magnetic flux of three phases must also be satisfied.

However, for a three-phase transformer, the magnetic flux of each phase is mutually coupled. So, when the residual flux is unknown, it is difficult to design the size of prefluxing current of each phase that can make the initial magnetic flux meet the symmetrical relationship requirement analyzed above. It will be further analyzed later. Therefore, this paper proposes the inrush current reduction strategy of ''phase-to-phase prefluxing and phase-to-phase controlled switching closing'', which avoids the problem of unknown residual flux through decoupling. The prefluxing speed mainly depends on the time constant of the prefluxing current. If the DC current source with a small time constant is selected, the entire closing process time will be short. The energization progress of transformer does not require high time requirement in fact. The basic process of the reduction strategy is shown in FIGURE 3. As for design of the key parameters such as prefluxing current, the prefluxing time, the closing time of each phase, etc. involved in the strategy will be further analysis.

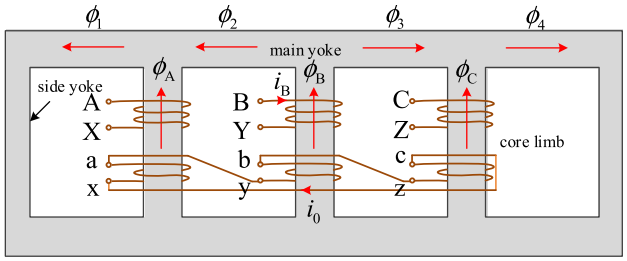

FIGURE 4. Three phases and five columns Y_0/Δ connection transformer structure diagram.

B. MAGNETIC CIRCUIT MODEL CONSTRUCTION AND MAGNETIC FLUX ANALYSIS

1) MAGNETIC CIRCUIT MODEL CONSTRUCTION

Transformer modeling mainly includes two methods: magnetic circuit and circuit [22]–[27]. In large-capacity transformers, there are mainly two types of cores: three phases and five columns type and three phases transformer with single phase core. Between them, the three phases and five columns core structure is more representative because it can reflect the mutual coupling of the three-phase magnetic flux.

The three phases and five columns transformer model is modeled from the perspective of the magnetic circuit is clear and intuitive, and the physical meaning of the parameter is clear. Furthermore, by setting the reluctance parameters in the magnetic circuit, the structure of the three phases transformer with single phase core can be reflected.

Therefore, the magnetic circuit of the three phases and five columns transformer is constructed to lay the foundation for the magnetic flux analysis.

The core structure of the three phases and five columns transformer and the winding connection mode of Y_0/Δ connection mode is shown in FIGURE 4. According to the electromagnetic field theory, the magnetic flux in the transformer core comes from the magnetomotive force generated by the winding currents of each phase. Assuming that the magnetomotive force in the three-phase primary winding is $F_A F_B F_C$, the magnetic flux in the three-phase core column, main yoke, and side yoke are as shown in the following figure.

Because of the secondary winding of the transformer is delta type, the winding will generate current due to electromagnetic induction when the three-phase magnetic flux is unbalanced. And each phase winding on the delta winding side flows the same magnitude zero-mode characteristic current, corresponding to the magnetomotive force F_0. According to Lenz's law, the magnetic flux generated by the induced current is opposite to the original zero-sequence magnetic flux, which plays a demagnetization effect.

Because the leakage inductance of the secondary side is small and the secondary winding is almost in a superconducting state, the induced current generated will almost completely cancel out the original zero-sequence magnetic flux, i.e., $\phi_A + \phi_B + \phi_C = 0$.

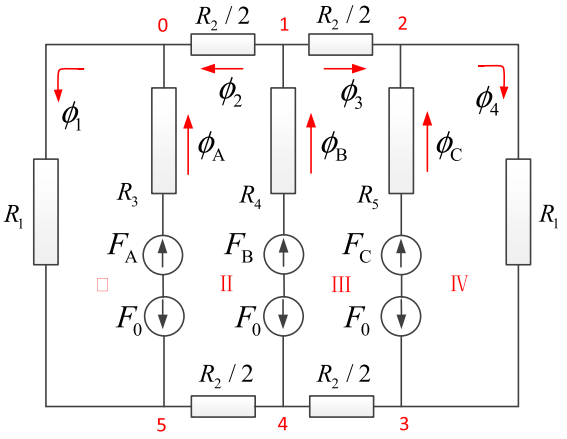

FIGURE 5. Three phases and five columns Y_0/Δ-connected winding transformer equivalent magnetic circuit.

When the iron core is not in a deep saturation state, the reluctance of the iron core will be much smaller than that of the air, so the magnetic flux is mainly concentrated in the iron core, and the leakage flux will be much less than that of the iron core. Therefore, the influence of leakage flux is ignored in the magnetic circuit modeling. The equivalent magnetic circuit diagram is constructed as shown in FIGURE 5 through the above analysis.

In the figure, R_3 R_4 R_5 are the reluctance of the ABC three phase cores, R_1 is the side yoke reluctance, and R_2 is the main yoke reluctance. When the core is not saturated, there is $R_5 = R_4 = R_3$. Each section of the core is made of the same material, so its reluctance is the ratio of the length of the magnetic circuit to the cross section, and is also related to the excitation characteristics of the core.

The magnetic flux generated by the magnetomotive force of each phase will be coupled to each other due to the connection of the iron core, so that R_1 and R_2 are not equal to 0 in the magnetic circuit correspondingly. If $R_1 = R_2 = 0$, and R_3 R_4 R_5 are the reluctance of each phase core of a three phases transformer with single phase core. The magnetic flux between phases can be seen as not coupled, and the magnetic circuit is equivalent to the magnetic circuit of a three phases transformer with single phase core. Therefore, the flux analytical expression of three phases and five columns transformer can be used to analyze three phases transformer with single phase core by setting $R_1 = R_2 = 0$.

According to Kirchhoff's current law, an equation that magnetic flux is the solution variable can be established by adopting the branch circuit analysis method.

$$\mathbf{GF} = \mathbf{\Phi} \tag{3}$$

Among them, in the magnetic circuit, $\mathbf{G}$ is the nodal admittance matrix of reluctance. Φ is the magnetic flux injected into each node. $\mathbf{F}$ is the magnetomotive force of each node, which is the variable to be solved. Where $\mathbf{\Phi} = \left[\frac{F_B-F_0}{R_4}, \frac{F_C-F_0}{R_5}, -\frac{F_C-F_0}{R_5}, -\frac{F_B-F_0}{R_4}, -\frac{F_A-F_0}{R_3}\right]'$, and then the

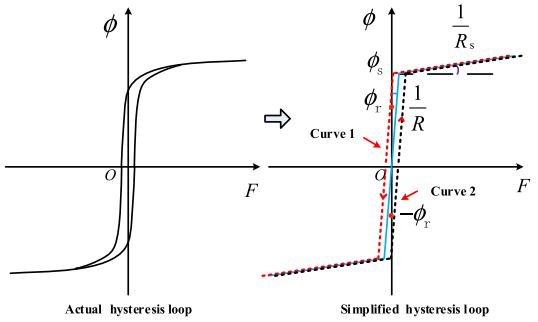

FIGURE 6. Iron core excitation characteristic curve.

three-phase core flux can be expressed as follows.

$$\begin{cases} \phi_A = \frac{F_5+F_A-F_0}{R_3} \\ \phi_B = \frac{F_4+F_B-F_1-F_0}{R_4} \\ \phi_C = \frac{F_3+F_C-F_2-F_0}{R_5} \end{cases} \tag{4}$$

According to the above analysis, there is equation below.

$$\phi_A + \phi_B + \phi_C = 0 \tag{5}$$

Core excitation characteristics is needed to be considered when solving the above equations. The core excitation characteristic $(\phi - i)$ has saturation and hysteresis characteristics, which can be described by a hysteresis loop model with more parameters. The corresponding reluctance R of each segment satisfies $R = Ni/\phi$. So it will also have saturation and hysteresis characteristics. The equivalent magnetic circuit actually contains multiple nonlinear elements, thus equation (3) is a nonlinear equation group. It is very difficult to obtain an analytical expression of the magnetic flux when the precise nonlinear characteristics of the iron core is considered. If only the numerical solution of the magnetic flux can be obtained, it is not conducive to grasping the changing law of the magnetic flux during the prefluxing and controlled switching process, and it is not conducive to the design of control parameters of the strategy. Therefore, it is necessary to obtain a simple and effective magnetic flux analytical expression as much as possible. In order to simplify the solution of magnetic flux, the actual hysteresis loop model can be simplified to a double broken line model based on the idea of piecewise linearity according to the IEC description method of core excitation characteristic, as shown by the blue line in FIGURE 6.

In order to describe the effect of residual flux, the double broken line is moved longitudinally. When the residual flux of the core is positive, the core characteristics are represented by the red curve 1. The corresponding characteristic equation is as follows:

$$\begin{cases} \phi = \frac{1}{R}F + \phi_r & -\phi_s \le \phi \le \phi_s \\ \phi = \frac{1}{R_s}\left(F - R\left(\phi_s - \phi_r\right)\right) + \phi_s & \phi > \phi_s \\ \phi = \frac{1}{R_s}\left(F + R\left(\phi_s - \phi_r\right)\right) - \phi_s & \phi < -\phi_s \end{cases} \tag{6}$$

When the residual flux of the core is negative, the core characteristics are represented by the black curve 2. The

corresponding characteristic equation is:

$$\begin{cases} \phi = \frac{1}{R}F - \phi_{\mathrm{r}} & -\phi_{\mathrm{s}} \le \phi \le \phi_{\mathrm{s}} \\ \phi = \frac{1}{R_s}\left(F - R\left(\phi_{\mathrm{s}} + \phi_{\mathrm{r}}\right)\right) + \phi_s & \phi > \phi_{\mathrm{s}} \\ \phi = \frac{1}{R_s}\left(F + R\left(\phi_{\mathrm{s}} + \phi_{\mathrm{r}}\right)\right) - \phi_s & \phi < -\phi_{\mathrm{s}} \end{cases} \tag{7}$$

In the formula, ϕ_{s} is the saturation magnetic flux of the iron core, R is the reluctance when iron core is not saturated, R_{s} is the reluctance when iron core is saturated, and there is $R_{\mathrm{s}} = u_r R$. When it is not saturated, the relative permeability of the iron core is very large, there is $u_r \approx 5000 - 8000$. The excitation characteristics of side yoke and the main yoke can also be described with the simplified excitation characteristics described above. After simplification, The analytic solution of equation group (3) can be obtained.

2) MODEL SOLUTION

In the process of designing the control parameters of the strategy, it is necessary to solve and analyze the magnetic flux. In different stages of the control process, the form of equations (3) and (5) remains unchanged, but the initial conditions of the equations will be different. Taking the prefluxing process of A-phase as an example, the magnetic flux of each phase is solved.

Because the A-phase is prefluxed, the initial conditions is that the residual flux of the three-phase core is ϕ_{Ar}, ϕ_{Br}, ϕ_{Cr}, and the residual flux of the side yoke and the main yoke are $\phi_{01\mathrm{r}}$ $\phi_{12\mathrm{r}}$ $\phi_{23\mathrm{r}}$ $\phi_{34\mathrm{r}}$ $\phi_{45\mathrm{r}}$ $\phi_{50\mathrm{r}}$ respectively. The subscript numbers represent the magnetic circuit node numbers.

A-phase is prefluxed at time 0, and the prefluxing current is I_{dA}. There is $F_{\mathrm{A}} = NI_{\mathrm{dA}}$, $F_{\mathrm{B}} = F_{\mathrm{C}} = 0$. Assuming that the prefluxing current does not reach the set value instantaneously, the form of prefluxing current is as follows:

$$I_{\mathrm{dA}} = I_{\mathrm{dAm}}\left(1 - e^{-\frac{t}{\tau}}\right) \tag{8}$$

where, τ is the time constant of prefluxing current, I_{dAm} is the amplitude of prefluxing current. When the core is not saturated, the analytical expression of three-phase magnetic flux is obtained by solving simultaneous equations(3)(5) as follows.

$$\begin{cases} \phi_A = -\frac{\sigma_1 + \sigma_2}{2\sigma_3} \\ \phi_{\mathrm{B}} = \frac{\sigma_4}{\sigma_5} \\ \phi_{\mathrm{C}} = -\frac{\sigma_6 + \sigma_7}{2\sigma_3} \end{cases} \tag{9}$$

where $\sigma_1 = NI_{\mathrm{dAm}}\left(3R_2 + 8R_3\right)\mathrm{e}^{-\frac{t}{\tau}}$, $\sigma_3 = R_2^2 + 5R_2R_3 + 6R_3^2$

$$\begin{aligned} \sigma_2 &= -\phi_{\mathrm{Ar}}\left(R_2^2 + 6R_2R_3 + 8R_3^2\right) + \left(\phi_{\mathrm{Br}} + \phi_{\mathrm{Cr}}\right) \\ &\quad - \left(R_2 + 2R_3\right)^2 NI_{\mathrm{dAm}}\left(3R_2 + 8R_3\right) \\ \sigma_4 &= -NI_{\mathrm{dAm}}\left(1 - e^{-\frac{t}{\tau}}\right) - \phi_{\mathrm{Ar}}R_3 + \phi_{\mathrm{Br}}\left(R_2 + 2R_3\right) \\ &\quad - \phi_{\mathrm{Cr}}R_3 \\ \sigma_5 &= R_2 + 3R_3 \\ \sigma_6 &= NI_{\mathrm{dAm}}\left(R_2 + 4R_3\right)\left(1\text{-}\mathrm{e}^{-\frac{t}{\tau}}\right) \\ \sigma_7 &= \left(\phi_{\mathrm{Ar}} + \phi_{\mathrm{Br}}\right)\left(R_2 + 2R_3\right)^2 - \phi_{\mathrm{Cr}}\left(R_2^2 + 6R_2R_3 + 8R_3^2\right) \end{aligned}$$

The analytical expression formula of A-phase magnetic flux is related to the prefluxing current, the unsaturated reluctance of the core and the residual flux of each phase, however it is not related to the residual flux of the side yoke and the main yoke through preliminary observation.

C. PARAMETER DESIGN AND MARGIN ANALYSIS OF INRUSH CURRENT SUPPRESSION STRATEGY

The basic idea of the prefluxing and controlled switching strategy has been described above. The focus now is to design the parameters in the strategy so that the magnetic flux of each phase can be within the saturated range during the entire closing process when applying strategy.

1) PREFLUXING CURRENT AND CLOSING TIME OF A-PHASE

A-phase is taken as the first closing phase. The key factors affecting the characteristics of A-phase magnetic flux are residual flux, prefluxing current and closing time. The size of the residual flux is not controllable, and only the parameters of the prefluxing current and closing time can be designed. In order to ensure that the core can be prefluxed to saturation under various residual flux modes, there must be a lower limit for the prefluxing current, denoted as I_{dAmL}, called the reference current. However, the iron core cannot be over saturated after prefluxing, otherwise it will produce large inrush current after closing. So, there is an upper limit of prefluxing current, which is recorded as I_{dAmH}. After prefluxing, σ_1 can be regarded as 0.

Equation (9) can be converted to equation (10).

$$I_{\mathrm{dAm}} = \frac{-\phi_{\mathrm{Ar}}\sigma_8 + \left(\phi_{\mathrm{Br}} + \phi_{\mathrm{Cr}}\right)\sigma_9 + 2\phi_{\mathrm{s}}\sigma_3}{\sigma_{10}} \tag{10}$$

where $\sigma_8 = R_2^2 + 6R_2R_3 + 8R_3^2$, $\sigma_9 = \left(R_2 + 2R_3\right)^2$, $\sigma_{10} = 3R_2 + 8R_3$

In any residual flux mode, it can be prefluxed to saturation flux, so the lower limit of prefluxing current should be the maximum value of I_{dAm}. In most cases, the residual flux of the transformer is generated when the circuit breaker is opened, so the magnetic fluxes at the three phases should satisfy the relationship of $\phi_{\mathrm{A}} + \phi_{\mathrm{B}} + \phi_{\mathrm{C}} = 0$. It is substituted in equation (10), I_{dAm} can be expressed as follows.

$$I_{\mathrm{dAm}} = \frac{2\left(R_2^2 + 5R_2R_3 + 6R_3^2\right)\left(\phi_{\mathrm{s}} - \phi_{\mathrm{Ar}}\right)}{N\left(3R_2 + 8R_3\right)} \tag{11}$$

It is easy to know that I_{dAm} can get the maximum when $\phi_{\mathrm{Ar}} = -0.85\phi_{\mathrm{m}}$.

$$\left(I_{\mathrm{dAm}}\right)_{\max 1} = \frac{3.5R_2^2 + 17.4R_2R_3 + 20.9R_3^2}{N\left(3R_2 + 8R_3\right)}\phi_s \tag{12}$$

The residual flux of the three-phase core of the transformer may not satisfy the sum of zero, such as after the DC resistance test. According to the relationship of the reluctance, when $\phi_{\mathrm{Ar}} = -0.85\phi_{\mathrm{m}}$, $\phi_{\mathrm{Br}} = \phi_{\mathrm{Cr}} = 0.85\phi_{\mathrm{m}}$, I_{dAm} achieves the maximum value:

$$\left(I_{\mathrm{dAm}}\right)_{\max 2} = \frac{4.2R_2^2 + 23.8R_2R_3 + 20.4R_3^2}{N\left(3R_2 + 8R_3\right)}\phi_s \tag{13}$$

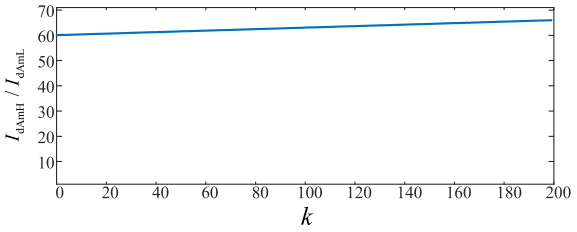

FIGURE 7. The relationship between I_{dAmH}/I_{dAmL} and k.

There is no doubt that $(I_{dAm})_{max\,2} \geq (I_{dAm})_{max\,1}$, because the latter residual flux mode already includes the mode where the sum of the three-phase residual flux is zero. So, there is $oI_{dAmL} = (I_{dAm})_{max\,2}$.

The final value of the magnetic flux is $n\varphi_s$ after prefluxing with the prefluxing upper limit current. Assuming $n = 1.05$ and $R_2 = kR_3$, the upper limit of prefluxing current can be resolved as:

$$I_{dAm} = \frac{\left[(2n+8)\,k^2+(7n+3)\,k+u_r\,(n-1)\,(3k+8)+4\right]\phi_s - \left(2k^2+10k+12\right)\phi_{Ar}}{(3k+8)\,N} R_3 \tag{14}$$

Further analysis of equation (14) shows that when the ratio k of the reluctance of the core column to the reluctance of the side yoke remains unchanged, both I_{dAmH} and I_{dAmL} are proportional to the reluctance R_3. Therefore, the ratio of I_{dAmH}/I_{dAmL} remains unchanged. For transformers with different core sizes, k may change, which may have a certain impact on the prefluxing current. The relationship between I_{dAmH}/I_{dAmL} and k is shown in FIGURE 7 when k is changed.

As it can be seen from the above figure, $I_{dAmH}/I_{dAmL}$is little affected by k. Actually, the commonly used core structure k does not exceed 10. At this time, I_{dAmH}/I_{dAmL} is basically maintained at 60 in size. When $k = 0$, it corresponds to the situation of three phases transformer with single phase core. At this time, there is also $I_{dAmH}/I_{dAmL} = 60$. Therefore, under different core structure types and core sizes, I_{dAmH}/I_{dAmL} is a very large value. It shows that the upper limit of prefluxing current is not high. The reason that there is such a wide range is mainly the saturation characteristics of the core itself. That is, after the magnetic circuit is saturated, the reluctance increases sharply. With only a modest flux increase beyond saturation, very high magnitude current pulses will be needed.

A certain type of 220kV three phases and five columns transformer is taken as an example to design the control parameters and analyze the parameter margin. The core material is a 0.3mm thick silicon steel sheet produced by Japan's Nippon Steel Corporation, and the basic parameters are shown in Figure 25 and Table 2.

Generally, the rated working magnetic density of iron core is 1.7T, and the saturation magnetic density is about (1.15 $\sim$ 1.25B_m). Here, 1.15 B_m is taken, i.e.,1.96T. When the actual parameters are taken into account, the solution can be obtained as follows:

TABLE 1. The influence of residual flux on different the inrush current reduction strategies.

Three-phase residual flux (pu)	The maximum amplitude of the inrush current								
	reference [1]			this paper			the control group		
	A	B	C	A	B	C	A	B	C
0 0 0	0.00	0.00	0.00	0.07	0.07	0.13	3.98	1.36	1.36
-0.7 0 0.7	0.14	0.53	0.41	0.07	0.07	0.13	7.96	1.59	5.25
-0.7 0.7 0	0.16	0.52	0.43	0.07	0.07	0.14	1.35	1.39	3.98
0.7 -0.7 0	0.14	0.53	0.41	0.07	0.08	0.15	0.25	0.18	1.28
0.7 0 -0.7	0.14	0.53	0.41	0.08	0.08	0.17	0.24	1.28	0.16
0 -0.7 0.7	0.32	1.40	1.11	0.07	0.07	0.13	4.14	0.52	5.10
0 0.7 -0.7	0.32	1.42	1.15	0.07	0.07	0.16	3.98	5.18	0.64
-0.35 -0.35 0.7	0.27	1.16	0.96	0.07	0.07	0.13	6.05	0.83	5.19

$$I_{dAmL}=12.2A \tag{15}$$

The reference current is about 1.93% of the rated current, closing to the rated excitation current, but far less than the rated current.

It can be seen from the above analysis that when the detailed parameters of transformer core are known, the current range required for prefluxing can be accurately calculated, and then the parameters of prefluxing equipment can be selected according to the actual situation. Even if the accurate core parameters cannot be obtained, because the reference current is close to the rated excitation current, and the prefluxing range is large, the median value of the range can be selected. That is to say that the DC current of 30 times the rated excitation current can be selected as the prefluxing current.

When the residual flux of A-phase is the worst, the reference current with the size of I_{dAmL} and a time constant of 5ms is used to preflux. The three-phase magnetic density B can be obtained by solving equation(9), as shown in FIGURE 6.

For transformers with different core structures, when the A-phase winding is prefluxed with reference current, the A-phase magnetic flux can reach the saturation value. So, the correctness of the prefluxing parameter design method is verified.

The closing time of A-phase is analyzed. When the A-phase prefluxing reaches the saturation value, the closing time of A-phase power supply is selected at phase 180 °. According to equation(2), the calculation equation of A-phase magnetic flux after closing is obtained.

$$\phi_A = \phi_m \cos(\omega t) + (\phi_s - \phi_m)\, e^{-\frac{R}{L}t} \tag{16}$$

It can be seen that the A-phase flux will not exceed the saturation value. Therefore, there is no inrush after A-phase closing. Therefore, the optimal closing angle of A-phase is

180 °. In order to shorten the closing time as far as possible, the corresponding optimal closing time t_A can be selected about two power frequency cycles after the completion of A-phase prefluxing.

In the actual situation, it is often impossible to achieve precise angle closing due to the dispersion of the breaker resulted from the wear of the mechanical breaking process and the influence of factors such as pre-breakdown. Under normal circumstances, the offset time caused by dispersion does not exceed ±1ms.

It is assumed that the A-phase offset angle is δ_1. According to equation (2), the aperiodic component of magnetic flux caused by offset is equation (17).

$$\phi_f = (\phi_r - \phi_m \cos(\delta_1)) e^{-\frac{R}{L}t} \tag{17}$$

Then the maximum magnetic flux after closing is as follows.

$$\phi_{max} = \phi_m + \phi_r - \phi_m \cos(\delta_1) \tag{18}$$

To achieve, through calculation, $-36° \leq \delta_1 \leq 36°$ must be met. In other word, if the offset time of the circuit breaker is within ±2ms, the magnetic flux can be controlled in the saturation range. Therefore, the dispersion of the closing time of the circuit breaker has little influence on the inrush current reduction effect under the strategy.

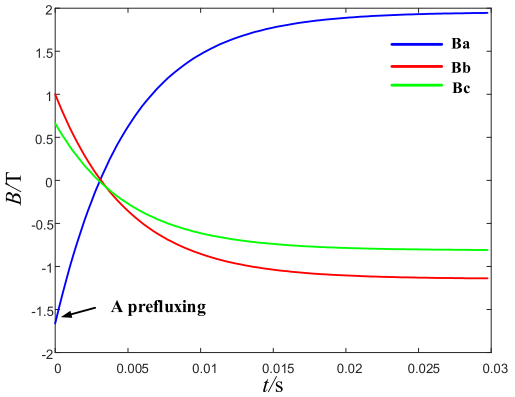

(a) Three phases and five columns type

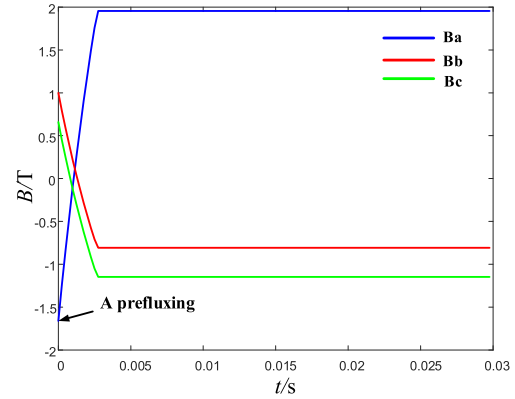

(b) Three phases transformer with single phase core structure

FIGURE 8. Three-phase magnetic density when A-phase is prefluxed.

2) PREFLUXING PARAMETERS AND CLOSING TIME OF B-PHASE

After the A-phase is closed, the B-phase and C-phase will produce induced magnetic flux due to coupling. The magnetic flux characteristics in the process of B-phase prefluxing and controlled switching are mainly affected by ''core flux equalization'' effect, A-phase magnetic flux, B-phase prefluxing current and prefluxing time, B-phase closing time, etc. These factors need to be analyzed one by one.

Analysis of the ''core flux equalization'' effect. The closing strategy based on the ''core flux equalization'' effect is proposed [1]. However, when the ''core flux equalization'' effect is not obvious, whether the strategy is applicable needed to be further analyzed.

If the initial magnetic flux of the B-phase and C-phase is different. The residual flux of B-phase is positive and C-phase is negative. After the A-phase is closed, the B-phase and C-phase will couple out the induced magnetic flux that follows the A-phase magnetic flux change. If the small hysteresis loop of the iron core has an obvious local saturation area as shown in FIGURE 9(a), the inductance at the beginning of B-phase is significantly greater than that of C-phase. In the transformer of Y_0/Δ connection mode, the same current will flow in the triangular winding, which will cause uneven voltage distribution on the BC phase winding. B-phase will induce a higher voltage due to higher inductance, so that the magnetic flux of B-phase increases rapidly, while the magnetic flux of C-phase changes slowly. Eventually the BC phase magnetic flux will be equal. This phenomenon is called the ''core flux equalization'' effect, which can quickly eliminate the influence of residual flux. If this phenomenon occurs in the core, the B-phase and C-phase flux will satisfy $\phi_B = \phi_C = -\frac{1}{2}\phi_A$. Therefore, it is thought that the best closing angle of B-phase and C-phase can be generated after two power frequency cycles after A-phase is closed [1], [19]. So controlled switching is adopted to reduce the inrush current of B-phase and C-phase effectively.

The above analysis shows that the condition for the production of the ''core flux equalization'' effect. The condition is that the generated small hysteresis loop has an obvious saturation section, such as the purple area in the B-phase and C-phase magnetic flux in FIGURE 9(a).

However, in fact, there is that the local small hysteresis loop saturation section is not obvious, when the core material does not undergo steady-state saturation. For example, the core material is a core material with low hysteresis loss, or the magnetic flux in the B-phase and C-phase is very small.

At this time, the excitation inductance of B-phase and C-phase is very large during the whole prefluxing process, and the ''core flux equalization'' effect will not be obvious, as shown in FIGURE 9 (b). At this time, after the closing of A-phase, the flux of B-phase and C-phase will be difficult to reach equilibrium. Therefore, the strategy based on the ''core flux equalization'' effect in references [1], [19] may fail, which is further demonstrated below.

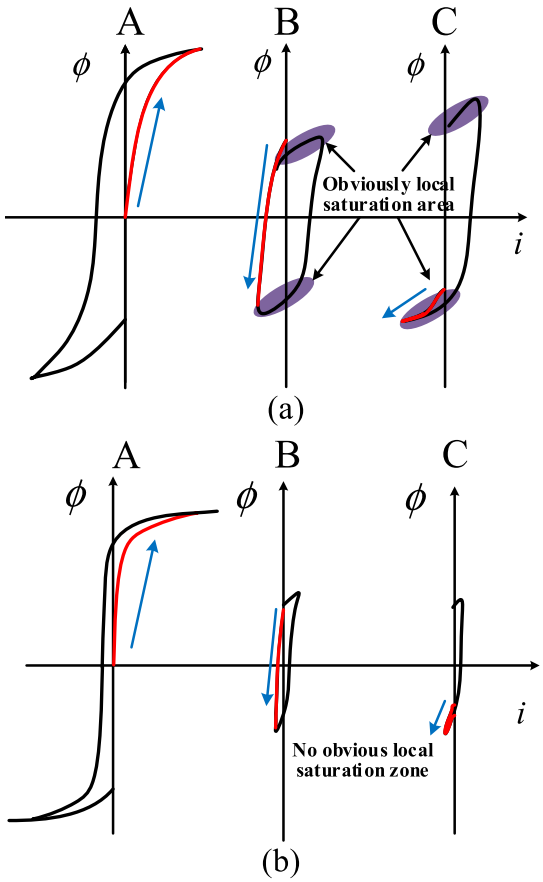

FIGURE 9. The "core flux equalization" effect of Y_0/Δ connection transformer.

The simplified hysteresis loop model is used to solve the magnetic flux of each phase after A-phase closing. After the closing of A-phase, the magnetic flux changes according to the sinusoidal law. So in the magnetic circuit model, the A-phase branch will become an equivalent current source, and there is $F_B = F_C = 0$. The equivalent magnetic circuit of three phases and five columns transformer is solved, and the results are shown in FIGURE 10. The induced magnetic flux of B-phase and C-phase is also changed according to the sine law, but the phase is opposite to that of A-phase. Obviously, the difference between B-phase and C-phase fluxes is very stable, and the ''core flux equalization'' effect is not obvious.

The magnetic flux of each phase after prefluxing is ϕ_{A1} ϕ_{B1} ϕ_{C1}. After prefluxing of A-phase, the magnetic flux change of each phase is analyzed, as shown in equation (19).

$$\begin{cases} \Delta\phi_{A1} = \phi_{A1} - \phi_{Ar} = \dfrac{NI_{dAm}\,(3R_2 + 8R_3)}{2\left(R_2^2 + 5R_2R_3 + 6R_3^2\right)} \\ \Delta\phi_{B1} = \phi_{B1} - \phi_{Br} = \dfrac{-NI_{dAm}}{R_2 + 3R_3} \\ \Delta\phi_{C1} = \phi_{C1} - \phi_{Cr} = -\dfrac{NI_{dAm}\,(R_2 + 4R_3)}{2\left(R_2^2 + 5R_2R_3 + 6R_3^2\right)} \end{cases} \tag{19}$$

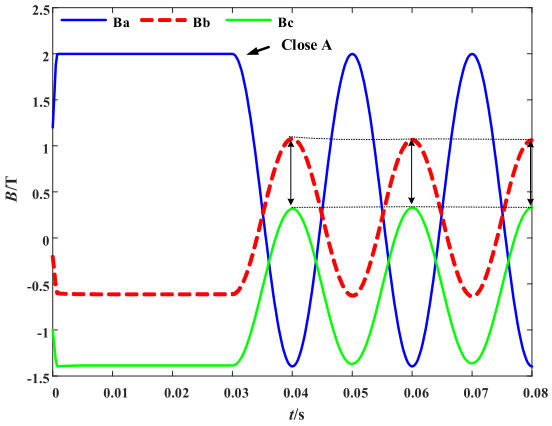

FIGURE 10. Three-phase magnetic flux during the prefluxing and controlled switching process of A-phase.

The ratio of the flux change of B-phase and C-phase to that of A-phase after prefluxing is as follows.

$$\begin{aligned} k_B &= \frac{\Delta\phi_{B1}}{\Delta\phi_{A1}} = -\frac{2R_2 + 4R_3}{3R_2 + 8R_3}, \\ k_C &= \frac{\Delta\phi_{C1}}{\Delta\phi_{A1}} = -\frac{R_2 + 4R_3}{3R_2 + 8R_3} \end{aligned} \tag{20}$$

It can be seen that k_B, k_C has nothing to do with the residual flux and prefluxing current of each phase, but only related to the relative ratio of reluctance. The result shows that the magnetic flux of B-phase and C-phase is related to the core reluctance and the initial residual flux of the three-phase when the A-phase is prefluxed. By analogy, it can be seen that the magnetic flux of B-phase and C-phase is closely related to the residual flux of each phase after A-phase is energized. Because of the randomness of residual flux, the optimal closing angle of the B-phase and C-phase will be difficult to determine. Therefore, the method of designing the optimal closing time based on the ''core flux equalization'' effect in reference is likely to fail [19], which will be verified in subsequent simulations. In order to solve the problem, the method that preflux the B-phase to the saturated magnetic flux to generate the optimal closing angle is proposed. This method is still applicable when the ''core flux equalization'' effect is not obvious.

Design the prefluxing parameters and closing time. It can be seen from FIGURE 10 that when the A-phase magnetic flux decreases, the B-phase magnetic flux increases. Therefore, when the A-phase magnetic flux is at the positive peak value and the B-phase is prefluxed, the superposition of the prefluxing effect and the magnetic flux interphase coupling effect will be more conducive to the saturation magnetic flux of the B-phase. and to the production of the optimal closing angle of the B-phase. Therefore, the optimal prefluxing time is the time when the A-phase magnetic flux is maximum, which corresponds to the 60° of B phase power.

The magnetic flux of B-phase prefluxing and closing process are solved and analyzed. Assume that the initial magnetic fluxes of the three phases before prefluxing of B-phase

are ϕ_{Ar2}, ϕ_{Br2}, ϕ_{Cr2}. From the analysis of the magnetic flux change of the A-phase prefluxing stage, it can be seen that before the B phase is prefluxed, even if ϕ_{Ar2} has been determined, the initial magnetic flux of the B-phase and C-phase is uncertain. The prefluxing time is t_{B1}. The deviation between the actual prefluxing time and the ideal prefluxing time is Δt (electrical angle is δ). The prefluxing current is I_{dB}, and $F_B = NI_{dB}$, $F_C = 0$. A-phase magnetic flux is a fixed value, see (16).

Refer to A-phase prefluxing parameter design conclusion, the characteristic of the B-phase core is the same as those of the A-phase. Therefore, when B-phase is prefluxed, the prefluxing current can also be chosen the same as A-phase. In this way, the parameters of the A-phase and B-phase prefluxing equipment can be exactly the same, which can simplify the prefluxing design process. The feasibility of this size of prefluxing current will be demonstrated below. Because the prefluxing process is relatively short, the magnetic flux attenuation is not considered in this process. The three-phase magnetic flux is resolved as follows:

$$\begin{aligned}\phi_A &= \phi_m \cos(\omega t + \delta) + \phi_s - \phi_m \\ \phi_B &= \phi_{FB} - (1-\sigma_8)\,\phi_m \cos(\omega t + \delta) - \sigma_8 \phi_m \cos\delta \\ &\quad + \phi_m - \phi_s - \phi_{Cr2} \\ \phi_C &= -\phi_{FB} + \sigma_8 \phi_m\,(\cos\delta) - \cos(\omega t + \delta)) + \phi_{Cr2} \qquad (21)\end{aligned}$$

Among them, $\sigma_8 = \frac{(R_2^2+4R_2R_3+4R_3^2)}{2R_2^2+9R_2R_3+8R_3^2}$, $\phi_{FB} = \frac{NI_{dAm}}{2R_3}\left(1\text{-}e^{-\frac{t}{\tau}}\right)$. σ_8 is a constant. ϕ_{FB} is the magnetic flux produced by the B-phase prefluxing current.

Because ϕ_{Br2} and ϕ_{Cr2} are both uncertain parameters, it is necessary to discuss whether magnetic flux of B-phase can meet the requirements of prefluxing to saturation under any ϕ_{Br2} and ϕ_{Cr2}. It can be seen from equation (21) that when ϕ_{Cr2} is the largest, the prefluxing speed of B-phase is the slowest, which is the least conducive to B-phase saturation. Because $\phi_{Br2} \geq -0.85\phi_s$ and the sum of the three-phase magnetic flux is 0, ϕ_{Cr2} gets the maximum,i.e., $\phi_{Cr2} = 0$ when $\phi_{Ar2} = 0$. Core parameters and prefluxing parameters are substituted to solve equation (21), the three-phase magnetic flux can be obtained as shown in FIGURE 11.

It can be seen that in the case where the initial residual flux has the most unfavorable effect, the B-phase magnetic flux can also be prefluxed to a saturation value within 5ms, and then maintain the saturation state for about 10ms. After this cycle, such a saturated state will circulate in each cycle. The phase angle of the B-phase voltage of 180° corresponds to t_{B2} just within the range of the saturation state of the phase. According to the equation (2), when the B-phase power supply is closed at t_{B2}, the B-phase iron core magnetic flux will not be saturated. So the B-phase hardly generates inrush current. In order to reduce the mutual interference between the prefluxing and controlled switching process, and to improve the efficiency of the closing process, it is considered to close B-phase within 1-2 cycles after the prefluxing. Of course, if the site does not require high closing time, the interval time

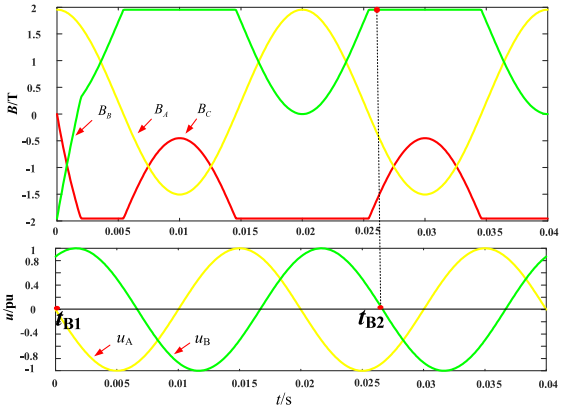

FIGURE 11. B-Phase prefluxing under the worst case of initial magnetic flux.

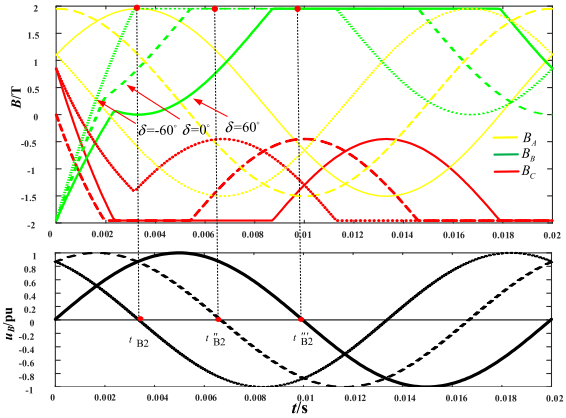

FIGURE 12. The influence of different prefluxing time on B-phase prefluxing.

can be delayed according to the actual situation. See the t_{B2} label in FIGURE 11.

The time margin of B-phase prefluxing is analyzed. The B-phase prefluxing process is simulated within $60° \leq \delta \leq 60°$, as shown in FIGURE 12.

It can be seen from the above that when the prefluxing angle deviation range is $-60° \leq \delta \leq 60°$, the $180°$(t'_{B2} t''_{B2} t'''_{B2} in the FIGURE 12) of B-phase power is within the B-phase magnetic flux saturation time interval. Therefore, under the larger error of prefluxing time, there is an optimal closing angle for B-phase.

Because the initial magnetic flux state during closing of B-phase is exactly the same as those of A-phase, the effect of the dispersion of the B phase breaker on the magnetic flux after closing is exactly the same as that of A-phase. Then the dispersion margin of the circuit breaker of this phase is consistent with the A-phase. Using the magnetic circuit parameters corresponding to the three phases transformer with single phase core, the magnetic flux in the B-phase prefluxing and controlled switching process of the structure transformer is solved and analyzed. It is found that the prefluxing parameters and prefluxing time of B-phase selected in

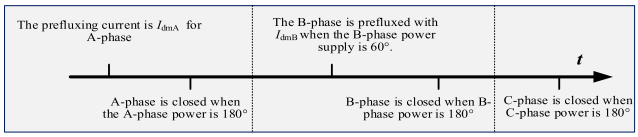

FIGURE 13. Inrush current reduction strategy based on the prefluxing and controlled switching.

the above-mentioned three phases and five columns structure transformer are also fully applicable to this structure. So, it will not be repeated here.

D. C-PHASE CLOSING TIME

After the A-phase and B-phase is closed, the magnetic flux of them is $\phi_A = \phi_m \cos(\omega t) + \phi_s - \phi_m$ and $\phi_B = \phi_m \cos(\omega t - 120°) + \phi_s - \phi_m$ respectively. Then due to the balance of the three-phase magnetic flux, the C-phase magnetic flux is solved as follows.

$$\phi_C = \phi_m \cos(\omega t + 120°) + 2\phi_m - 2\phi_s \tag{22}$$

Because $\phi_s = 1.15\phi_m$, the maximum amplitude of C-phase magnetic flux is $1.13\phi_s$. Therefore, the C-phase magnetic flux will be slightly saturated. However, it can be seen from equation (22) that the C-phase magnetic flux induced makes the C-phase induced voltage completely equal to the C-phase power supply voltage before the C-phase is closed. Therefore, the inrush current generated by the C-phase circuit breaker closed is the same at any closing time. Then is no need to preflux C-phase. The closing angle of B-phase is consistent with A-phase and B-phase, i.e., the C-phase power supply is closed at 180°. The closing time t_C of C-phase can is selected 1-2 cycles delay from the closing of B-phase.

The silicon steel sheet 30Z120 produced by Nippon Steel has a rated magnetic density of 1.7T and a maximum core residual flux of 1.4T. The initial residual flux coefficient (the ratio of the initial residual flux to the magnetic flux at the time of breaker opening) is about 82%. The steady-state residual flux coefficient (the ratio of steady-state residual flux to initial residual flux) is approximately 80% [15]. When the magnetic flux is prefluxed to saturation, the prefluxing current is removed, and the residual flux is about 1.3T. Therefore, when using this prefluxing strategy and considering the attenuation characteristics of residual flux, the magnetic density will exceed the saturation magnetic density by 0.1T. There will be very weak saturation, but no large inrush current will be generated.

Based on the above analysis of magnetic flux, the key control parameters in the strategy are designed. The summary of the entire prefluxing and controlled switching process is shown in FIGURE 13.

III. SIMULATION VERIFICATION AND EFFECTIVENESS ANALYSIS

Based on the simplified magnetic circuit model, the magnetic flux is analyzed and the reduction strategy of inrush current

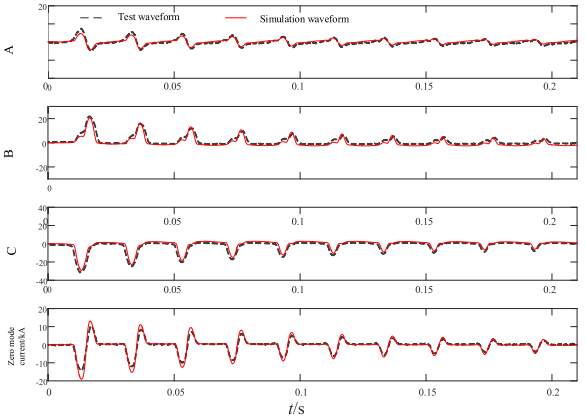

FIGURE 14. Transformer simulation model verification.

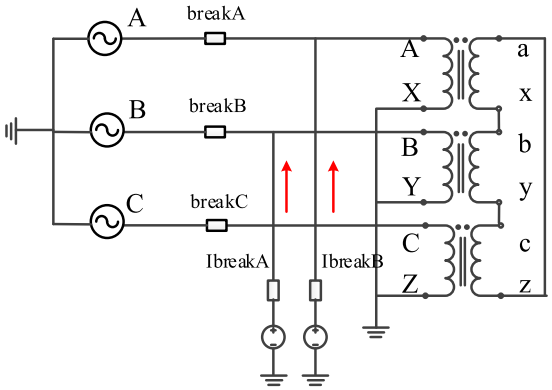

FIGURE 15. The prefluxing and controlled switching circuit.

is proposed in above. Based on PSCAD, this section will verify the accuracy of the theoretical analysis and analyze the influence of different factors on the strategy effect.

A. VERIFICATION OF MODEL ACCURACY

PSCAD is a widely used electromagnetic transient simulation platform. The classic transformer model in PSCAD can simulate magnetic flux leakage and loss. The latest version can use the widely recognized J-A model to describe the core hysteresis characteristics and residual flux. In order to accurately reflect the inrush current characteristics of transformer in simulation, the different layout of transformer windings is considered and the model by parameter compensation is further improved [29]. The accuracy of the improved model was verified by dynamic simulation tests. The same simulation model as the dynamic simulation system is built. A closing angle of 90° and a power supply voltage of 790V is chosen. The simulation and test waveforms obtained are shown in the figure below.

It can be seen that the simulated waveform and the test waveform are in good agreement, and the same phenomenon occurs at other closing angles and power supply voltages. Therefore, the improved model can be used to accurately simulate the magnetic flux in the three-phase core.

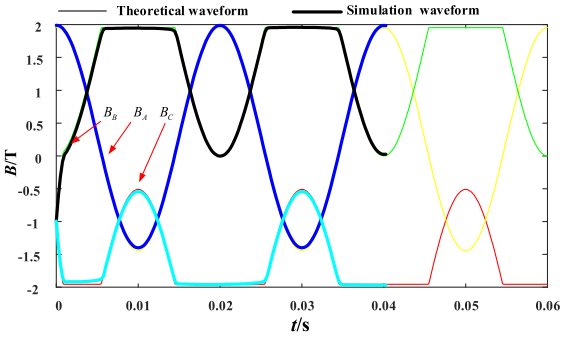

FIGURE 16. Comparison of magnetic flux theory and simulation solution in strategy.

From the time of A-phase closing to the B-phase prefluxing, the magnetic flux of the iron core was solved theoretically and simulated separately. The prefluxing and controlled switching circuit used in the simulation is shown in FIGURE 15. The basic parameters such as transformer short-circuit impedance are shown in Table 2. Before B-phase prefluxing, set the initial magnetic density of the three phases is 1pu −0.5pu −0.5pu, and the prefluxing current is 12.2A. The results of the two methods are shown in FIGURE 16.

It can be seen from the comparison in FIGURE 16, the magnetic flux solved by the simulation changes more smoothly at the inflection point of the magnetization curve. This is caused by the use of the J-A model in the simulation model. However, the magnetic flux obtained by the simplified magnetic circuit and the magnetic flux obtained by the accurate simulation have a very high degree of fit, which verifies the accuracy of the magnetic flux analysis method proposed in this paper.

B. THE INFLUENCE OF DIFFERENT FACTORS ON THE STRATEGY EFFECT

1) THE "CORE FLUX EQUALIZATION" EFFECT

Reference [1] uses the "core flux equalization" effect to find the optimal closing angle under the condition of known the residual flux of A-phase. In fact, for different core materials, the "core flux equalization" effect is also different. It is convenient to simulate the hysteresis loops of iron cores of different materials by setting the parameters of the J-A model. Thereby, different types of "core flux equalization" effect can be simulated. It is found through simulation that the "core flux equalization" effect is more obvious when the core loss is high. At this time, the inrush current reduction strategy proposed in reference [1] and the strategy proposed in this article both have great effect. The maximum amplitude of the inrush current does not exceed 0.01pu, shown as follows.

However, when the core loss is small, the "core flux equalization" effect is not obvious, and the magnetic flux of B-phase and C may not be balanced for a long time. Set the three-phase initial residual flux to 0.7pu −0.35pu −0.35pu and the comparison of the reduction effects of the two strategies is shown in FIGURE 18. It can be seen that when the

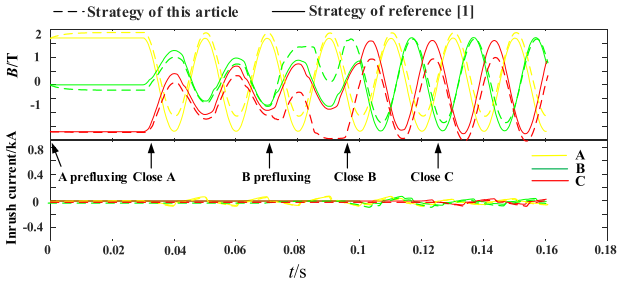

FIGURE 17. Comparison of inrush current reduction effects of the two strategies under the obvious "core flux equalization" effect.

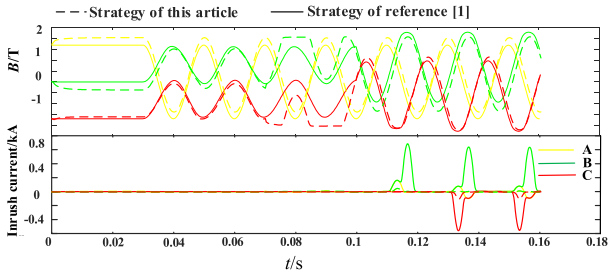

FIGURE 18. Comparison of inrush current reduction effects of the two strategies when the "core flux equalization" effect is not obvious.

strategy proposed in reference [1] is adopted, the maximum inrush current reaches more than 0.6pu. But when the strategy proposed in this paper is adopted, the maximum inrush current is only 0.1pu.

2) TYPICAL RESIDUAL FLUX

In the above theoretical analysis, the inrush current reduction strategy proposed in this paper considers the worst case of residual flux when calculating the prefluxing current. To verify its effectiveness, sets of typical residual flux combinations are set up below, and the simulation results are shown in TABLE 1.

It can be seen from TABLE 1 that when there is no inrush current reduction measure, the maximum value of inrush current is random, and the maximum can reach 8 pu. When adopting the strategy proposed in reference [1], the maximum value of inrush current is nearly 1.4 pu, but with the change of residual flux, the maximum value of inrush current fluctuates greatly. After adopting the inrush current reduction strategy based on the prefluxing and controlled switching proposed in this paper, the maximum value of inrush current does not exceed 0.5 pu, which is very stable and not affected by residual flux.

3) PREFLUXING TIME

Theoretical analysis shows that when the deviation between the actual prefluxing time and the ideal prefluxing time is within the range of (−60°, 60°), there is an optimal closing angle for B-phase. FIGURE 19 shows the inrush current under different deviations obtained through simulation.

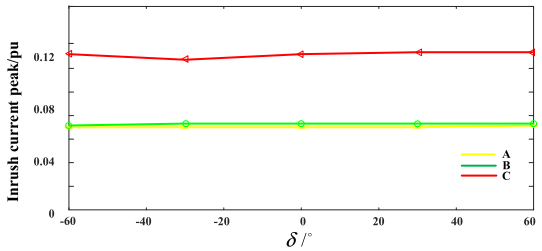

FIGURE 19. The influence of the angle deviation of B-phase prefluxing on inrush current reduction effect.

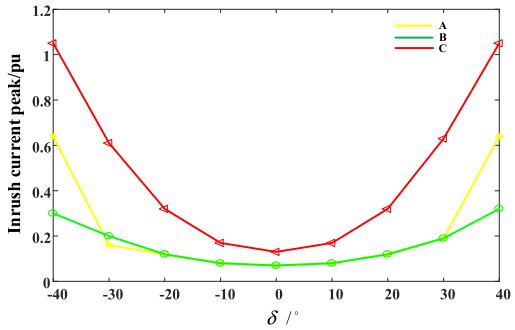

FIGURE 20. The influence of the dispersion of circuit breakers on inrush current reduction effect.

It can be seen from FIGURE 19 that when the deviation angle is within the range of $(-60°, 60°)$, the three-phase inrush current is kept at a very small value.

4) THE DISPERSION OF CIRCUIT BREAKER

Theoretical analysis points out that when $-36° \leq \delta_1 \leq 36°$, the dispersion of the circuit breaker has little effect on the inrush current reduction. The simulation result is shown in FIGURE 20.

It can be seen from FIGURE 20 that the magnitude of the inrush current has a parabolic relationship with the error angle of the circuit breaker. As the error angle of the circuit breaker increases, the maximum of the inrush current will increase. But as long as it stays within the range of $(-40°, 40°)$, the maximum of the three-phase inrush current will not exceed the rated current, which verifies the correctness of the above theoretical analysis and shows that the strategy proposed in this paper has greater tolerance to the dispersion of circuit breakers.

In summary, in the case of different residual flux combinations, considering the dispersion of the circuit breaker, the reduction strategy proposed in this paper has a significant inrush current reduction effect, which has obvious advantages compared with the common controlled switching inrush current reduction strategy.

IV. ANALYSIS ON THE IMPROVEMENT OF PROTECTION PERFORMANCE BY STRATEGY

Differential protections of transformer itself and the adjacent components may malfunction because of the large inrush current or the corresponding inrush current generated during the energization of the transformer. And the unbalanced component in the inrush current may cause the zero-sequence protection of the transformer itself and adjacent components to malfunction. Under the strategy proposed in this article, the inrush current can be effectively reduced, which can avoid the problem of related protection malfunction or miss trip caused by the inrush current, thereby improving the protection performance. Taking the transformer differential protection as an example, the analysis is as follows.

As the main protection of the transformer, the differential protection can quickly remove the fault within tens of milliseconds when the fault occurs, and provide reliable protection to the transformer. And its malfunction should be avoided as much as possible when the transformer is closed.

In engineering, restraint criteria such as the 2nd harmonic restraint criteria is widely used to achieve this goal. However, when the transformer is energized to a small turn-to-turn fault, the current in the closing circuit is dominated by inrush current, which makes the fault characteristics very weak. Due to the existence of the restraint criteria, the differential protection is still braked, and the fault can only be removed after the inrush current decays to a small value. The fault has further developed, and the time to remove the fault is basically more than 100 milliseconds, causing serious damage to the transformer and threatening the safe and stable operation of the power grid.

The influence of the paper's strategy on the differential protection when the transformer is energized in no-fault and small inter-turn fault condition will be analyzed as follows.

A. CLOSED IN NO FAULT CONDITION

In the prefluxing stage, according to the parameter design analysis, the prefluxing current will be much smaller than the rated current. The operating threshold of the transformer differential protection setting is generally greater than 0.2 times the rated current. Therefore, the differential protection will not malfunction during the prefluxing process.

In the closing phase after the prefluxing is completed. When there is no fault, each phase of the core magnetic flux can be prefluxed to saturation value. Therefore, when the closing angle is 180°, the iron core will not be deeply saturated, thereby the inrush current can be effectively reduced and the differential protection will not malfunction.

B. CLOSED IN SMALL INTER-TURN FAULT CONDITION

For the prefluxing process, it can be seen from the previous analysis that the prefluxing current will not exceed the differential protection threshold value, so the protection will not operate. Because the prefluxing current is too small, it will not have a bad effect on the prefluxing equipment and the transformer, even if the protection does not operate.

For the closing process, because the strategy in this article uses single-phase prefluxing and single-phase closing, a single-phase circuit can be used to analyze the prefluxing and controlled switching process. Take A-phase fault analysis as

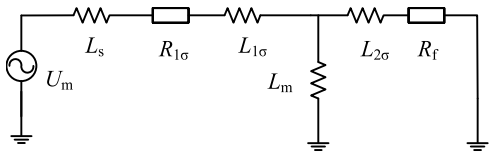

FIGURE 21. Closing circuit corresponding to A-phase turn-to-ground fault.

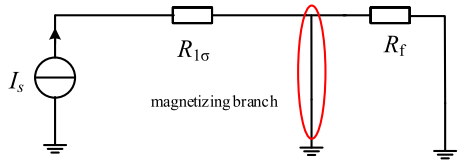

FIGURE 22. Prefluxing circuit in the case of A-phase turn-to-turn fault.

an example. There are two main types of weak internal faults in the transformer: turn-to-turn fault and turn-to-ground fault. The turn-to-turn fault can be converted into a turn-to-ground fault for analysis [30]. So the fault characteristics of turn-to-ground fault is mainly analyzed.

When a turn-to-ground fault occurs, the no-load transformer becomes an autotransformer with a load. The load is the transition resistance. The closing circuit is shown in FIGURE 21.

To analyze the magnetic flux of the transformer under the strategy of this article, and then analyze the fault characteristics and its impact on the protection. According to formula (2), the A-phase magnetic flux of closing after prefluxing is as follows:

$$\phi_{\mathrm{A}} = \phi'_{\mathrm{m}} \cos(\omega t) + \left(\phi_{\mathrm{z}} - \phi'_{\mathrm{m}}\right) \mathrm{e}^{-\frac{R}{L}t} \tag{23}$$

ϕ_{z} is the magnetic flux after prefluxing of A-phase, and ϕ'_{m} is the steady-state magnetic flux after closing.

The magnetic flux composition is further analyzed. During prefluxing process, since the prefluxing current is DC the prefluxing current is mainly distributed according to the resistance. At this time, the prefluxing branch is in a short-circuit state, as shown in FIGURE 22.

Therefore, the prefluxing current will all flow through the excitation branch, which is the same as the prefluxing situation when there is no fault. According to the linear relationship between magnetic flux and current, there are:

$$\phi_{\mathrm{z}} = \phi_{\mathrm{s}} \tag{24}$$

After the A-phase is closed, the steady-state excitation current is $\dot{I}'_{\mathrm{m}}$. According to closing circuit showed in FIGURE 22, $\dot{I}'_{\mathrm{m}}$ can be obtained as follows:

$$\dot{I}'_{\mathrm{m}} = \frac{\left(R_{\mathrm{f}} + j\omega L_{2\sigma}\right) // j\omega L_{\mathrm{m}}}{j\omega\left(L_{\mathrm{s}} + L_{1\sigma}\right) + R_{1\sigma} + \left(R_{\mathrm{f}} + j\omega L_{2\sigma}\right) // j\omega L_{\mathrm{m}}} \cdot \times \frac{\dot{U}_{\mathrm{m}}}{j\omega L_{\mathrm{m}}} \tag{25}$$

Among them, R_{f} is the transition resistance of the turn-to-ground fault. It has been converted to the value of the primary side.

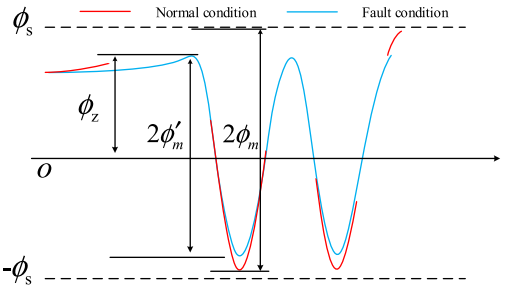

FIGURE 23. Magnetic flux during the prefluxing and controlled switching process under normal and fault conditions.

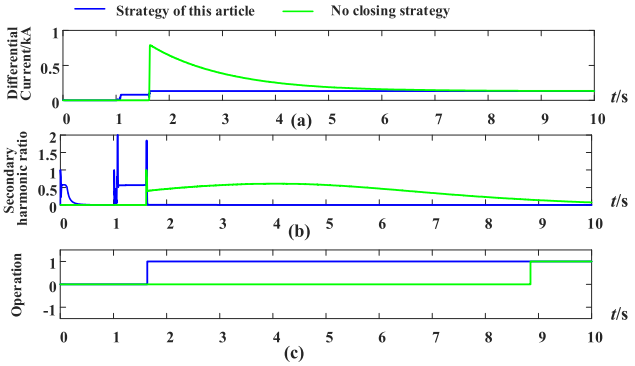

FIGURE 24. With or without inrush reduction strategy, the protection operation when the transformer is energized in small turn-to-ground fault condition.

Assuming that when the transformer is operating normally, the steady-state magnetic flux amplitude is ϕ_{m}, corresponding to the steady-state excitation current $\dot{I}_{\mathrm{m}}$. $\dot{I}_{\mathrm{m}}$ can be obtained as follows:

$$\dot{I}_{\mathrm{m}} = \frac{j\omega L_{\mathrm{m}}}{j\omega\left(L_{\mathrm{s}} + L_{1\sigma}\right) + R_{1\sigma} + j\omega L_{\mathrm{m}}} \cdot \frac{\dot{U}_{\mathrm{m}}}{j\omega L_{\mathrm{m}}} \tag{26}$$

Due to $R_{1\sigma} \ll \omega\left(L_{\mathrm{s}} + L_{1\sigma}\right)$, and $\left|\left(R_{\mathrm{f}} + j\omega L_{2\sigma}\right) // j\omega L_{\mathrm{m}}\right| < \omega L_{\mathrm{m}}$, $\left|\dot{I}'_{\mathrm{m}}\right| < \left|\dot{I}_{\mathrm{m}}\right|$ can be analyzed according to formulas(25)(26). According to the linear relationship between magnetic flux and current, there must be $\phi'_{\mathrm{m}} < \phi_{\mathrm{m}}$.

The above analysis shows that if there is a prefluxing and controlled switching strategy, the maximum value of the positive magnetic flux of the A-phase is also ϕ_{s}. So the iron core will not be positively saturated.

According to equation (23), the minimum value of magnetic flux after closing is $\phi_{\mathrm{z}} - 2\phi'_{\mathrm{m}}$. According to $\phi_{\mathrm{m}} \approx 0.87\phi_{\mathrm{s}}$ and $\phi'_{\mathrm{m}} < \phi_{\mathrm{m}}$, there must be $(\phi_{\mathrm{z}} - 2\phi'_{\mathrm{m}}) > -\phi_{\mathrm{s}}$, so the iron core will not be negative polarity saturated.

FIGURE 23 shows the comparison of the magnetic flux changes between normal and fault conditions when both use this closing strategy. It can be seen that after adopting this strategy, the iron core will not be saturated during the whole process of transformer closing, and the transformer closing circuit will be exactly the same as the circuit when the transformer is short-circuited during steady-state operation.

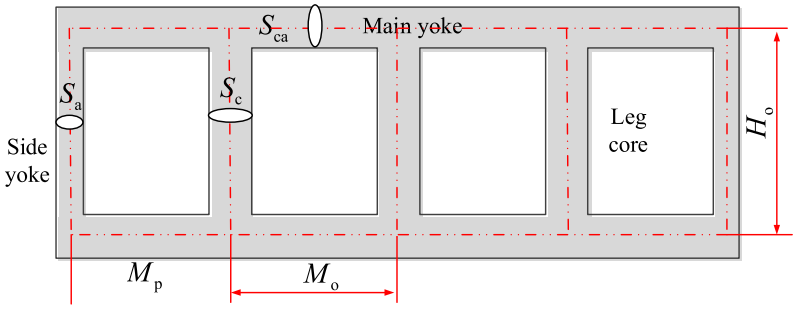

FIGURE 25. Schematic of 220kV three phases and five columns transformer core size.

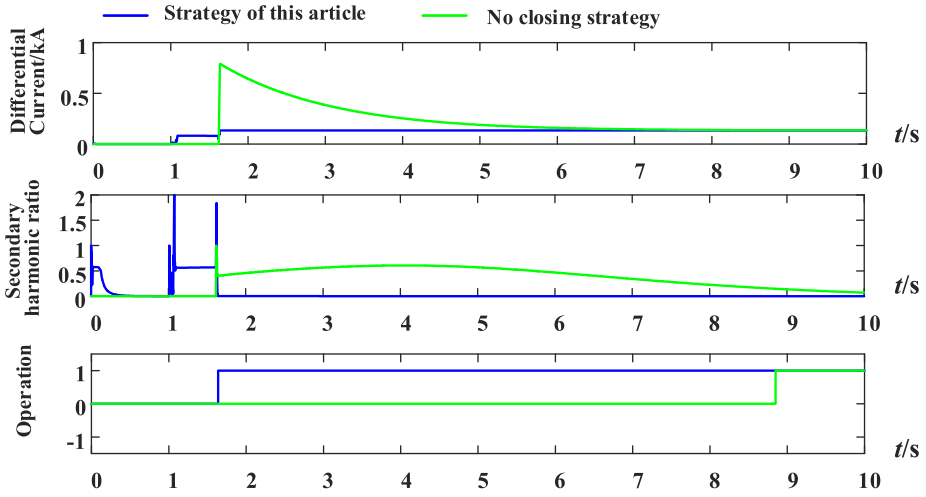

FIGURE 26. Turn-to-ground fault protection operation when closing at 22% turns ratio.

TABLE 2. 220kV three phases and five columns transformer core size.

Core size	H_o(mm)	M_o(mm)	M_p(mm)	S_c(cm^2)	S_a(cm^2)	S_{ca}(cm^2)
Size	2 230	1 930	1 270	7180.5	3420.4	3834.8

TABLE 3. Electromagnetic parameters of a typical 220kV three phases and five columns transformer.

Capacity/kVA		240/240/80
Voltage level/ kV		220/115/10.5
Rated current/A		629.8/1024.9/4398.9
Rated excitation current/%		0.067
Load loss/kW	H-M	637.38
	H-L	193.80
	M-L	184.09
NO-Load loss/kW	/	96.5
Short circuit impedance/%	H-M	13.65
	H-L	36.41
	M-L	20.64

Therefore, the nature and size of the fault current generated by the two working condition should also be the same. That is, its second harmonic ratio is low, and the differential protection will not be braked due to closing. It's verified by simulation as follows.

C. VERIFIED BY SIMULATION

Set a small turn-to-ground fault on the primary side of the transformer for simulation. The short-circuit turns ratio is 4.5%, and the transition resistance is 2Ω. The simulation result is shown in the figure below.

It can be seen that the fault current is very slight, about $0.15I_N$, but it exceeds the protection operation threshold. When adopting this strategy, there is almost no inrush current, and the protection can instantly remove the fault. When there is no inrush current reduction strategy, the three phases will be closed at random residual flux and random angles. The transformer will generate a large inrush current. The second harmonic attenuation is relatively slow. So, the protection is to be braked for a long time. The fault can be removed after at least 7s. Other turns ratio simulation is shown in Figure 25. It all shows that when there is the strategy, the differential protection can also operate faster when the transformer is energized in the small turn-to-ground fault condition.

In summary, the simulation analysis shows that when the prefluxing and controlled switching strategy is adopted in this paper, even if the transformer is closed to a slight fault, the transformer core will not be saturated. The inrush current can be effectively reduced, and the slight fault characteristics can be well reserved. Therefore, for differential protection, the protection can trip quickly, which improves the sensitivity and quick operation of the protection.

V. CONCLUSION

Based on the principle of inrush current reduction, this paper proposes the inrush current reduction strategy of based on the prefluxing and controlled switching technology. By constructing an equivalent magnetic circuit model suitable for large-capacity transformers, an analytical expression of the magnetic flux when implementing the strategy is obtained. Based on the analysis, the design method of the control parameters such as the prefluxing current and the optimal closing angle of each phase power supply is given. The influence of factors such as the dispersion of the circuit breaker, the deviation of prefluxing time and the residual flux on the reduction effect of the strategy is comprehensively analyzed. Finally, through accurate inrush current simulation, the correctness and superiority of the strategy are explained. The results show that the strategy has the following characteristics:

1) The proposed strategy is suitable for three phases transformer with five columns core or single phase core. In fact, it is also applicable to transformers such as three phases and three columns structure transformer. It is only need to change the boundary conditions to design specific parameters.

2) The required basic prefluxing current is small, and the current selection range is large. At 1 to 60 times the prefluxing reference current, the magnetic flux can be prefluxed to an ideal saturation state.

3) Not affected by residual flux and ''core flux equalization'' effect, this strategy can reduce the inrush current to less than 0.5 times the rated current under any working conditions where residual flux and ''core flux equalization'' effect are not obvious.

4) It has good tolerance to the deviation of prefluxing time and the dispersion of circuit breakers, which improves the possibility of strategic engineering application.

5) This strategy can still reduce the inrush current well when the transformer is energized in the small turn-to-ground fault condition. So, the sensitivity and speed of operation of related protections such as differential protection can be improved effectively.

APPENDIX

See Figure 25 and 26.
See Table 2 and 3.

REFERENCES

[1] J. H. Brunke and K. J. Frohlich, ''Elimination of transformer inrush currents by controlled switching—Part I: Theoretical considerations,'' *IEEE Trans. Power Del.*, vol. 16, no. 2, pp. 281–285, Apr. 2001.

[2] J. H. Brunke and K. J. Frohlich, ''Elimination of transformer inrush currents by controlled switching—Part II: Application and performance considerations,'' *IEEE Trans. Power Del.*, vol. 16, no. 2, pp. 276–280, Apr. 2001.

[3] J. H. Brunke, ''Elimination of transient inrush currents when energizing unloaded power transformers,'' Ph.D. dissertation, Swiss Federal Inst. Technol., Portland State Univ, Zürich, Switzerland, 1998.

[4] X. Qi, X. Yin, Z. Zhang, D. Chen, Y. Wang, and F. Cai, ''Study on the unusual misoperation of differential protection during transformer energization and its countermeasure,'' *IEEE Trans. Power Del.*, vol. 31, no. 5, pp. 1998–2007, Oct. 2016.

[5] W. Cao, X. Yin, Z. Zhang, Y. Pan, Y. Wang, and X. Yin, ''Characteristic analysis of zero-mode inrush current of high-impedance transformer,'' *Int. J. Electr. Power Energy Syst.*, vol. 117, May 2020, Art. no. 105716, doi: 10.1016/j.ijepes.2019.105716.

[6] C. Li, N. Zhou, and Q. Wang, ''A method to eliminate transformer inrush currents using soft-starter-based controlled energization,'' *Trans. China Electrotech. Soc.*, 10.19595/j.cnki.1000-6753.tces.190996.

[7] P. Liu and C. Huang, ''An adaptive blocking scheme for magnetizing inrush current in distribution lines,'' *Trans. China Electrotech. Soc.*, vol. 34, no. 11, pp. 2395–2404, 2019.

[8] E. Cardelli, E. D. Torre, V. Esposito, and A. Faba, ''Theoretical considerations of magnetic hysteresis and transformer inrush current,'' *IEEE Trans. Magn.*, vol. 45, no. 11, pp. 5247–5250, Nov. 2009, doi: 10.1109/TMAG.2009.2031084.

[9] P. C. Y. Ling and A. Basak, ''Investigation of magnetizing inrush current in a single-phase transformer,'' *IEEE Trans. Magn.*, vol. 24, no. 6, pp. 3217–3222, Nov. 1988.

[10] N. Chiesa and H. K. Høidalen, ''Novel approach for reducing transformer inrush currents: Laboratory measurements, analytical interpretation and simulation studies,'' *IEEE Trans. Power Del.*, vol. 25, no. 4, pp. 2609–2616, Oct. 2010, doi: 10.1109/TPWRD.2010.2045772.

[11] J. H. Brunke and K. J. Frohlich, ''Elimination of transformer inrush currents by controlled switching. II. Application and performance considerations,'' *IEEE Trans. Power Del.*, vol. 16, no. 2, pp. 281–285, Apr. 2001, doi: 10.1109/61.915496.

[12] D. I. Taylor, N. Fischer, J. D. Law, and B. K. Johnson, ''Using LabVIEW to measure transformer residual flux for inrush current reduction,'' in *Proc. 41st North Amer. Power Symp.*, Oct. 2009, pp. 1–6.

[13] D. Cavallera, V. Oiring, J.-L. Coulomb, O. Chadebec, B. Caillault, and F. Zgainski, ''A new method to evaluate residual flux thanks to leakage flux, application to a transformer,'' *IEEE Trans. Magn.*, vol. 50, no. 2, pp. 1005–1008, Feb. 2014, doi: 10.1109/TMAG.2013.2282175.

[14] D. I. Taylor, J. D. Law, B. K. Johnson, and N. Fischer, ''Single-phase transformer inrush current reduction using prefluxing,'' *IEEE Trans. Power Del.*, vol. 27, no. 1, pp. 245–252, Jan. 2012, doi: 10.1109/TPWRD.2011.2174162.

[15] L. Jia, S. Ma, and Z. Li, ''Research on initial residual flux coefficient and stable residual flux coefficient of current transformer,'' *Hydropower Energy Sci.*, vol. 35, no. 11, pp. 194–197, 2017.

[16] J. Xu *et al.*, ''Experimental research on inrush current suppression of unloaded transformers based on the controlled switching,'' *Power Syst. Protection Control*, vol. 46, no. 8, pp. 135–141, 2018.

[17] H. Ni, S. Fang, and H. Lin, ''A simplified phase-controlled switching strategy for inrush current reduction,'' *IEEE Trans. Power Del.*, vol. 36, no. 1, pp. 215–222, Feb. 2021, doi: 10.1109/TPWRD.2020.2984234.

[18] S. Fang, H. Ni, H. Lin, and S. L. Ho, "A novel strategy for reducing inrush current of three-phase transformer considering residual flux," *IEEE Trans. Ind. Electron.*, vol. 63, no. 7, pp. 4442–4451, Jul. 2016, doi: 10.1109/TIE.2016.2540583.
[19] J. Mitra, X. Xu, and M. Benidris, "Reduction of three-phase transformer inrush currents using controlled switching," *IEEE Trans. Ind. Appl.*, vol. 56, no. 1, pp. 890–897, Jan. 2020, doi: 10.1109/TIA.2019.2955627.
[20] Y. Cui, S. G. Abdulsalam, S. Chen, and W. Xu, "A sequential phase energization technique for transformer inrush current reduction—Part I: Simulation and experimental results," *IEEE Trans. Power Del.*, vol. 20, no. 2, pp. 943–949, Apr. 2005, doi: 10.1109/TPWRD.2004.843467.
[21] W. Xu, S. G. Abdulsalam, Y. Cui, and X. Liu, "A sequential phase energization technique for transformer inrush current reduction part II: Theoretical analysis and design guide," in *Proc. IEEE Power Eng. Soc. Gen. Meeting*, Jun. 2004, p. 534.
[22] B. A. Mork, F. Gonzalez, D. Ishchenko, D. L. Stuehm, and J. Mitra, "Hybrid transformer model for transient simulation—Part I: Development and parameters," *IEEE Trans. Power Del.*, vol. 22, no. 1, pp. 248–255, Jan. 2007, doi: 10.1109/TPWRD.2006.883000.
[23] B. A. Mork, "Five-legged wound-core transformer model: Derivation, parameters, implementation and evaluation," *IEEE Trans. Power Del.*, vol. 14, no. 4, pp. 1519–1526, Oct. 1999, doi: 10.1109/61.796249.
[24] X. Chen, "A three-phase multi-legged transformer model in ATP using the directly-formed inverse inductance matrix," *IEEE Trans. Power Del.*, vol. 11, no. 3, pp. 1554–1562, Jul. 1996.
[25] M. Nagpal, T. G. Martinich, A. Moshref, K. Morison, and P. Kundur, "Assessing and limiting impact of transformer inrush current on power quality," *IEEE Trans. Power Del.*, vol. 21, no. 2, pp. 890–896, Apr. 2006, doi: 10.1109/TPWRD.2005.858782.
[26] R. Yacamini and A. Abu-Nasser, "The calculation of inrush current in three-phase transformers," *IEE Proc. B Electr. Power Appl.*, vol. 133, no. 1, p. 31, 1986.
[27] B. A. Mork, F. Gonzalez, D. Ishchenko, D. L. Stuehm, and J. Mitra, "Hybrid transformer model for transient simulation—Part II: Laboratory measurements and benchmarking," *IEEE Trans. Power Del.*, vol. 22, no. 1, pp. 256–262, Jan. 2007, doi: 10.1109/TPWRD.2006.882999.
[28] C. Baozhi, "Selection of the cross-sectional area of the main yoke and side yoke of the three-phase five-column transformer," *Transformer*, vol. 42, no. 7, pp. 13–18, 2005.
[29] Y. Pan, X. Yin, W. Cao, Y. Chen, X. Yin, Y. Wang, and Q. Guo, "Simulation modeling of high impedance transformer based on PSCAD with deep correlation of winding structure," in *Proc. IEEE Innov. Smart Grid Technol.-Asia (ISGT Asia)*, May 2019, pp. 1187–1192.
[30] X. Deng, "Research on new protective algorithm and development of digital relay for power transformer," Ph.D. dissertation, School Elect. Electron. Eng., Huazhong Univ. Sci. Technol., Wuhan, China, 2011.

YUANLIN PAN was born in Sichuan, China, in 1993. He received the B.S. degree from Chongqing University, Chongqing, China, in 2016. He is currently pursuing the Ph.D. degree in power electrical engineering with the Huazhong University of Science and Technology. He research interest includes relay protection of AC and DC power grid research.

XIANGGEN YIN (Member, IEEE) received the B.S., M.S., and Ph.D. degrees in electrical engineering from the Huazhong University of Science and Technology (HUST), Wuhan, China, in 1982, 1985, and 1989, respectively. He is currently a Professor with the School of Electrical and Electronic Engineering, HUST. His research interests include fault location, protective relaying, and power system stability control.

ZHE ZHANG received the Ph.D. degree in electrical engineering from the Huazhong University of Science and Technology (HUST), Wuhan, China, in 1992. He is currently a Professor with the College of Electrical and Electronic Engineering, HUST. His research interests include power system analysis and protective relaying.

BINYAN LIU received the B.S. degree from Chongqing University, Chongqing, China, in 2019. He is currently pursuing the M.S. degree in power electrical engineering with the Huazhong University of Science and Technology. His research interest includes protective relaying.

MAOLIN WANG received the B.S. degree from Chongqing University, Chongqing, China, in 2018. He is currently pursuing the M.S. degree with the Huazhong University of Science and Technology. His current research interests include protective relaying and power system stability control.

XIN YIN (Member, IEEE) received the B.Eng. degree in electronic engineering from The University of Sheffield, U.K., in 2008, the M.Sc. degree in telecommunications from University College London, U.K., in 2009, and the Ph.D. degree in electrical and electronic engineering from The University of Manchester, U.K., in 2016. He is currently a Postdoctoral Research Associate of Electrical Engineering with the University of Liverpool. His current research interests include distribution systems and microgrid control with renewable energy.